Direction-Selective Resistance to Cerebrospinal-Fluid Flow As the Generative Mechanism of Syringomyelia

Han Soo Chang, M.D.

Department of Neurosurgery, Tokai University
Isehara, Japan

ABSTRACT

The pathophysiology of syringomyelia is not well understood. Current theories cannot explain a common mechanism for different types of syringomyelia. Especially, they cannot explain how cerebrospinal fluid (CSF) enters from low-pressure subarachnoid space to high-pressure syrinx and remains inside. We approached this problem with a computer simulation of the CSF flow in the spine. We hypothesized as follows. Suppose there is a direction-selective CSF resistance at some point in the subarachnoid space. A to-and-fro CSF movement across it will produce an alternating asymmetric pressure gradient inside the spinal cord, which subsequently drives the CSF in the intraspinal channel in the resisted direction.

We constructed a model of CSF dynamics in the spine, an electric circuit based on a lumped parameter model with multiple compartments. We then placed a direction-selective resistance in the subarachnoid space so that it would resist only the caudal flow. We analyzed the model's response to the to-and-fro CSF movement.

The to-and-fro CSF movement across the resistance produced a sustained pressure elevation in the caudal intraspinal channel. This phenomenon did not occur if the inserted resistance was bidirectional. The detailed mechanism was as follows. Caudal flow across the direction-selective resistor produced a pressure drop in the caudal subarachnoid segment, subsequently decreasing the spinal-channel pressure there. The resulting pressure gradient in the spinal channel drove CSF caudally. Because this phenomenon did not occur in the rostral flow phase, the rostral flow in the channel during this phase was smaller. Overall, each cycle of to-and-fro CSF movement pumped some CSF caudally in the spinal channel.

Our hypothesis provides a common mechanism for different types of syringomyelia and explains how CSF is driven to the syrinx against the pressure gradient.

Introduction

The pathophysiology of syringomyelia is still poorly understood. Many hypotheses exist in the literature[1–13], but they provide widely different explanations on the mechanisms of syrinx generation. We may, however, enumerate what few consensuses as follows. First, the syrinx fluid is identical to the CSF, and there is some communication between the syrinx and the subarachnoid space. Many studies support this point[14–17], albeit some different opinions[13,18]. Second, some derangement of CSF flow in the spinal subarachnoid space causes syrinx both in Chiari-I malformation[7,19–22] and subarachnoid arachnopathy[23–26]. Notably, the cerebellar tonsil deranges the CSF flow in the former and adhesive arachnoiditis in the latter.

The problem, however, is where this communicating channel resides and what mechanism generates the syrinx. On these points, there is no solid experimental or clinical evidence, and the opinions of researchers vary widely. Gardner et al.[1] thought that the central canal intercommunicates the syrinx and the fourth ventricle. Arterial pulses then exert pressure waves on the central canal and generate the syrinx. Williams et al. also postulated the communication through the central canal. He, however, emphasized the craniospinal pressure gradient produced by Valsalva maneuver et al.[2].

On the other hand, Ball and Dayan[4] assumed that CSF entered the syrinx through the perivascular space of arteries penetrating the spinal cord. This idea has the following variations. Heiss et al.[7] proposed that the piston-like movement of the cerebellar tonsils in Chiari-I patients generated pressure waves in the spinal subarachnoid space. And it subsequently drove CSF into the syrinx through the perivascular space. Stoodley et al. also considered the perivascular space as the communicating channel, but he assumed the arterial pulse pressure as the driving force[27]. All these assumptions are not proven and remain hypothetical. Although recent researchers seem to favor the perivascular-space theory, there remains the possibility that a thin communicating channel exists between the syrinx and the fourth ventricle[28].

In our opinion, the main theoretical problems reside in the following points.

1. No theory can explain the pathophysiological mechanism of syringomyelia in a unified fashion.

2. No theory can explain how CSF enters from the low-pressure subarachnoid space to the high-pressure syrinx cavity and remains inside.

As to the first point, there are different syringomyelia types, such as Chiari-I-malformation and spinal-arachnopathy-related[23]. The Chiari-I-malformation-related syringomyelia is further divided into communicating and non-communicating[29]. Current theories cannot explain these different types of syringomyelia in a unified fashion. However, it may be more natural to conjecture some common mechanism underlying these different types of syringomyelia[27]. The second point is theoretically essential but challenging. Physical laws dictate that the expanded syrinx cavity has higher pressure than the subarachnoid space[7,30–32]; the inside pressure must additionally confront the elastic tension of the syrinx wall. Therefore, merely assuming a communicating channel does not explain how CSF enters the syrinx against this pressure gradient and remains inside. Even if we take a specific time window where the subarachnoid pressure exceeds the syrinx pressure, it does not explain how the CSF remains inside the syrinx after it.

The current article is part of our effort to solve the above theoretical problems. We proposed in our previous paper[28] a hypothesis on the pathophysiology of syringomyelia. We hypothesized that a direction-selective resistance to spinal subarachnoid CSF flow causes syringomyelia. Suppose there is a resistance to spinal CSF flow only in the, e.g., caudal direction. To-and-fro CSF movement across it will pump CSF in an intraspinal channel caudally, causing syringomyelia. This hypothesis seemed to solve the two problems listed above. However, in that article, we just drew a rough sketch of this process and left out a detailed explanation. The current article will describe this mechanism in detail using computer simulation.

For this purpose, we used a mathematical model simulating the CSF movement of the spine. We revised a lumped parameter model with multiple compartments used in our previous articles[11,12]. We placed a direction-selective resistance in this model at a certain point in the spinal subarachnoid space. We then observed how it affected the CSF flow in the channel inside the spinal cord.

Material and Method

There is a problem when we try to simulate the motion of biological fluids such as blood and CSF. Such bodily fluids move inside flexible tubes. It differs from the usual situation of fluid mechanics, where the boundary of the fluid conduit is solid. Thus, we cannot simply apply the standard Navier-Stokes equations for our simulation. For this reason, researchers have commonly used lumped parameter models[33,34]. This model considers the fluid flow inside a flexible tube analogous to the electric flow in an electric circuit. The accumulation of electricity in a capacitor represents the expansion of a flexible tube and the accompanying pressure elevation. An electrical resistor represents the frictional resistance to flow. This model has a wide variety. For example, it may model the whole cardiovascular system as one electric circuit, or it may model it as a synthesis of multiple compartments of electric circuits[33,34]. Our current model is the type of lumped parameter model with multiple compartments that simulates the CSF dynamics in the spine and is an updated version of the model used in our previous articles[11,12]. We did not intend to make a quantitatively precise model of the spinal CSF flow but to make a basic model that could reveal the phenomenon underlying the generation of syringomyelia.

Previously, we developed a mathematical model that simulated the CSF flow in the spine[11,12]. This model (a multiple-compartment version of a 1-dimensional lumped parameter model) could describe the CSF movement in the whole spine (Figure 1). This model assumed an intraspinal CSF channel—the central canal or some other equivalent channel. In this model, the D capacitors represented the dural tension, C capacitors the tension of the central canal, R resistors the frictional resistance in the subarachnoid space, and r resistors the frictional resistance in the central canal.

Figure 2 shows the bare electric circuit extracted from Figure 1. A set of differential equations could describe the behavior of this model. Using computer software, we could numerically calculate its behavior in response to a certain cranial pressure wave (defined as a boundary condition on the cranial nodes). The concrete parameters were determined as follows.

- We increased the number of compartments from 10 to 100, thereby making the model more precise.
- We set the length of the modeled spinal cord to be 1 meter.
- The resistance of the subarachnoid space (R) was estimated using the following equations of Poisseuille[35–37].

$$\Delta P = \frac{8\pi\mu LQ}{A^2} = RQ$$

  - ΔP: Pressure difference between the adjacent compartments
  - Q: flow speed per unit surface

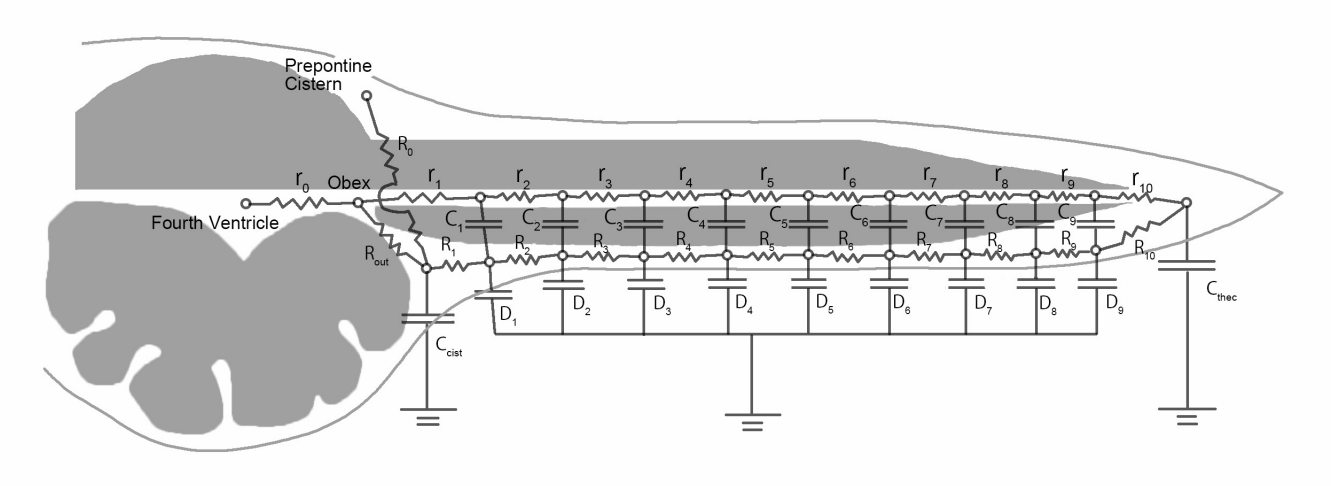

Figure 1. Schema of the electric circuit model of the CSF dynamics in the spine.

- μ: viscosity coefficient. In this case, it was set to the value of water (0.0007).
- L: distance between the adjacent compartments. It was set to 1 cm.
- A: cross sectional area of the subarachnoid space. It was set to the value of a concentric annulus[37] with the outer diameter of 1cm and the inner diameter of 0.7 cm ($1.6 \times 10^{-4}(m^2)$)

Thus, R was calculated to be 6872 $(Pa \cdot sec/m^3)$

- The resistance of the central canal (r) was estimated using the same equation with A set to $\pi(10^{-4})^2$ (m^2), i.e. the cross sectional area of a tube with a diameter of 100 μm. Thus, r was calculated to be 1.78×10^{11} $(Pa \cdot sec/m^3)$
- We determined the capacitance (C_{sub})corresponding to the dural elasticity so that the pressure-wave velocity determined by the time constant (RC) will roughly correspond to the pressure-wave velocity of the downward CSF wave observed in phase-contrast MRI of normal individuals. Thus, we set $C_{sub} = 0.1$ $(m^3/Pa \cdot sec)$.

Figure 1 shows the scheme of the constructed electric circuit model. This model represents the CSF movement in the spine as electric flow through multiple compartments of capacitances connected with resistors. A set of differential equations can describe the behavior of this electric circuit, and we can solve it numerically by setting the voltage at the cranial nodes as the boundary condition (Figure 2). In the previous articles[11,12], we only analyzed the transient behavior of the model to a sudden pressure increase on the cranial side of the subarachnoid space. This analysis helped simulate the situation of coughing or Valsalva maneuvers. In this article, however, we analyzed the response of the model to an oscillating cranial pressure wave simulating the normal cardiac pulsation of the CSF.

We numerically solved the differential equations using computer software (Mathematica version 12, Wolfram Research, Champaign, IL, U.S.A.) on a personal computer. We set the boundary conditions as follows. (1) The voltage at the two cranial nodes was set to a sine wave oscillating around 10 cmH_2O with an amplitude of 20 cmH_2O at one cycle per second. (2) The initial dural pressure was set at 10 cmH_2O in all segments. We set the step of the numerical solution to 1/5000 second and calculated the solution from zero to 20 seconds. The actual Mathematica codes can be found in our GitHub repository (https://github.com/chang-hs/syrinx_simulation.git).

We analyzed the original normal system and two of its modifications. In the first modification, we simply increased the subarachnoid resistance at point 25 (R_{25}) by 20 times. In the second modification, we placed a direction-selective subarachnoid resistance at point 25, so that only the resistance to the caudal flow would be increased by 20 times.

Results

We present the systems' responses to twenty cycles of to-and-fro waves in animations. The x-axis of each animation represents the 100 nodes of the circuit laid out from the cranial to caudal direction. The y-axis displays some of the following four measures: the dural tension (voltage in D capacitors in Figure 2), the canal tension (voltages in C capacitors), the subarachnoid

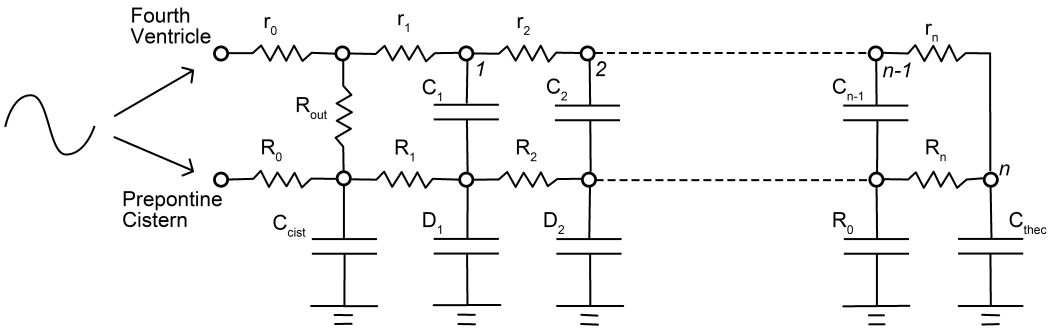

Figure 2. Electric circuit diagram representing the CSF dynamics of the spine

CSF flow (flows in R resistors), and the channel flow (flows in r resistors). We plotted the caudal flow in the positive and the rostral flow in the negative direction. The pressure values are shown in cmH_2O, the flows in ml/sec. To plot the four measures in a single animation, we multiplied the following three measures—the canal tension, the subarachnoid CSF flow, and the canal flow—with the following coefficients, respectively: namely, the canal tension with 50, the subarachnoid flow with 0.005, and the canal flow with 1.5×10^5.

Video 1 shows the original system's response representing the normal condition. In this state, the dural tension made a smooth gradient along the spine, whose polarity alternated along the pressure cycle. According to this pressure gradient, CSF made a smooth to-and-fro movement in the subarachnoid space with the corresponding pressure wave along the dura and the central canal. CSF also made smooth to-and-fro movements in the channel. There was almost no pressure elevation in the intra-spinal channel.

In Video 2, we increased the subarachnoid resistance R_{25} by 20 times, thereby simulating a simple block of the subarachnoid flow in both directions. In this condition, both the caudal and rostral flow across the resistance produced pressure drop in the distal subarachnoid segment. This pressure drop caused an increase in canal flow in the same direction as the subarachnoid flow. This increased canal flow caused a transient increase in the canal pressure distal to the block and a decrease proximal to the block. However, these pressure changes alternated along the alternation of the flow direction and did not produce a sustained pressure increase.

In Video 3, we replaced the subarachnoid resistor R_{25} with a direction-selective resistor whose resistance to the rostral flow was unchanged but that to the caudal flow was increased by 20 times. This time, sustained high pressure appeared in the intra-spinal channel in the segment distal to the replaced resistor, and sustained low pressure in the segment proximal to it. This sustained pressure gradually accumulated as the flow cycle proceeded. The dural tension showed a pressure drop at node 25 only during the caudal-flow phase. The to-and-fro canal flow increased near the node 25 similarly to that in the simple block above, but, this time, the increase was larger in the caudal direction.

We extracted the canal flow from this animation and showed it in Video 4. Observing this video, we can see that the cumulative total of the caudal flow is larger than that of the rostral flow, meaning that the CSF is virtually pumped caudally at node 25. To further elucidate this point, Video 4 simultaneously shows the canal flow in the simple block as shown in Video **??** and that in the one-way block as shown in Video **??**. We can clearly see that the caudal flow is about the same in the two models, while the rostral flow is smaller in the direction-selective model. It means that CSF in the intra-spinal channel is pumped caudally in each cycle of the to-and-fro CSF movement.

Discussion

In this article, we theoretically analyzed the CSF movement in the spine using a lumped parameter model with multiple compartments. It simulated a system with an elastic tube (dura) containing an elastic cylindrical material (spinal cord) that itself had a fluid channel inside. When we placed a direction-selective resistor in the subarachnoid space and evoked a to-and-fro pressure wave on this system, it produced a sustained pressure elevation in the segment distal to the resistor in the resisted direction. This phenomenon may explain the pathogenesis of syringomyelia both in Chiari I malformation and syringomyelia associated with arachnopathy.

Subarachnoid pressure pushes the spinal cord material and affects the pressure inside the intra-spinal channel. As seen in Figure 2, the absolute pressure inside the intra-spinal channel is the sum of the subarachnoid and channel tension (voltages of C_k and D_k in electrical terms). Suppose a one-way valve selectively resists caudal flow in the subarachnoid space at point A. Caudal CSF flow creates a pressure drop across point A, with the caudal pressure smaller than the proximal one. Thus, the absolute pressure in the canal distal to point A become smaller because the outside subarachnoid pressure there is smaller. It, therefore, creates a pressure gradient in the central canal across point A, thereby increasing the distal CSF flow in the canal at that point (Figure 3).

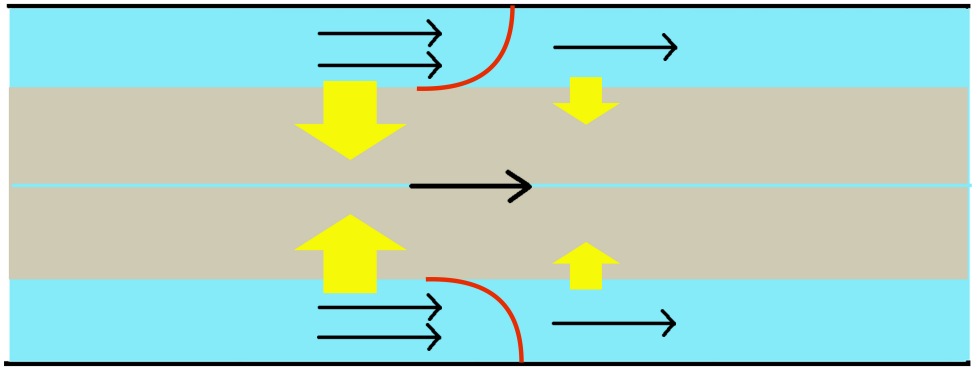

Figure 3. Increased central-canal flow across a direction-selective resistance in the subarachnoid space

On the contrary, rostral flow, not encountering resistance, does not create a pressure drop (Figure 4). Although some of the CSF that had been pumped caudally during the caudal-flow phase will flow back rostrally, its amount will be smaller. The net result will be that some CSF is pumped caudally in one cycle of the to-and-fro movement. Thus, CSF gradually accumulates in the distal segment of the resistance (Video 3). We hypothesize that this is the mechanism underlying the syrinx generation.

This theory successfully explains how CSF is pumped against the pressure gradient and remains inside the syrinx, one of the problems pointed out in the Introduction. A one-way valve in subarachnoid space creates an asymmetry of the pressure gradient between the caudal and rostral flow phases in the central canal. This asymmetric alternation of pressure gradient effectively pumps CSF caudally, creating sustained pressure elevation in the caudal segment. In other words, the energy of the to-and-fro CSF movement is translated via the one-way valve into the creation and sustenance of syringomyelia.

Direction-selective resistance to CSF flow is not an imaginative assumption. In Chiari-I malformation, the herniated tonsils move like a ball-valve; they are displaced caudally during the caudal flow and rostrally during the rostral flow. The higher velocity observed in the phase-contrast MRI studies suggests that they selectively impede the caudal CSF flow more than the cranial flow. Williams et al. demonstrated direction-selective resistance at the craniovertebral junction of Chiari-I patients, which became the basis of his theory[38]. Also, some types of arachnoid pathology may function as one-way valves. In 2014,

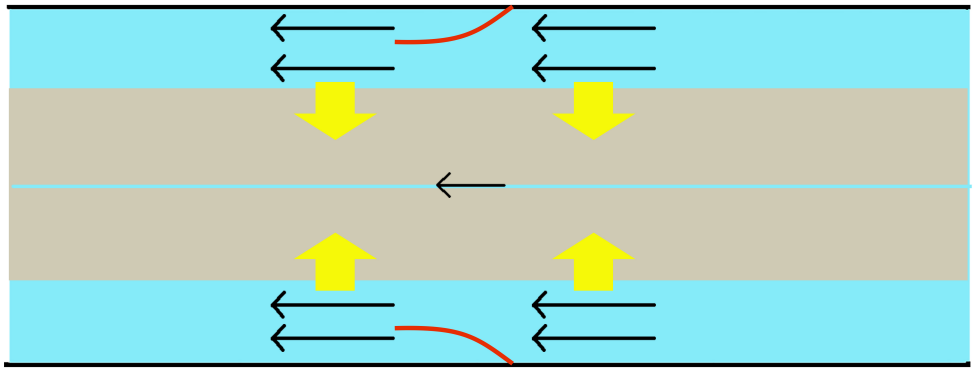

Figure 4. Normal central-canal flow across a direction-selective resistance during the reverse flow

we reported cases of thoracic arachnoid web associated with syringomyelia, in which phase-contrast MRI demonstrated one-way-valve-like behavior of the arachnoid web[26]. In surgery, we found an obliquely oriented arachnoid web that resembled a one-way valve. Thus, our hypothesis may also solve the second theoretical problem we pointed out in the Introduction. Namely, the direction-selective resistance in spinal subarachnoid space may function as the common mechanism underlying both Chiari-I-related and arachnopathy-related syringomyelia.

Our theory clearly explained how the energy of the to-and-fro CSF movement was transformed into the energy-requiring CSF trasport into the syrinx. However, previous theories seemed to have difficulty in explaining this process. According to the theories of Heiss et al.[7] or that of Stoodley et al.[27], the energy is provided by either enhanced pressure waves in subarachnoid space or pulsation of spinal arteries. However, none of these theories explains the detailed mechanism

Our restuls may cast some light on another interesting question. In cervical spondylosis, subarachnoid space is similarly obliterated by the protruding discs and osteophytes. Although this is a widely prevaent disease, we rarely encounter syringomyelia associated with cervical spondylosis. In our results, a simple block of the subarachnoid CSF flow did not produce sustained elevation of intraspinal channel pressure (Video 2). This result may explain why syringomyelia is rarely associated with cervical spondylosis.

There are some controversial points in our theory. Our model presumed the existence of a CSF channel inside the spinal cord. It may be controversial because most syringes seem to lack such communication. Yet, there still may exist a narrow CSF channel that is undetectable on MRI. In fact, ordinary MRI does not visualize the central canal with a diameter of 100 micrometers. Therefore, assuming the existence of a CSF channel inside the cord will not be far-fetched. Another point of controversy will be the role of the central canal. The human central canal is obstructed with advancing age, and assuming a function of the central canal may not befit that fact. However, the obliteration of the central canal seem to be a slow process, and it could be mostly patent up to the fourth decade[39,40]. Moreover, the CSF channel does not have to be the central canal but some other channel created inside the spinal cord matrix.

References

1. Gardner, W. J. & Angel, J. The mechanism of syringomyelia and its surgical correction. *Clin Neurosurg.* **6**, 131–40 (1958).

2. Williams, B. On the pathogenesis of syringomyelia: A review. *J. Royal Soc. Medicine* **73**, 798–806 (1980).

3. Milhorat, T. H. *et al.* Chiari I malformation redefined: Clinical and radiographic findings for 364 symptomatic patients. *Neurosurgery* **44**, 1005–1017, DOI: 10.1097/00006123-199905000-00042 (1999).

4. Ball, M. J. & Dayan, A. D. Pathogenesis of syringomyelia. *Lancet (London, England)* **2**, 799–801, DOI: 10.1016/s0140-6736(72)92152-6 (1972).

5. Klekamp, J. The pathophysiology of syringomyelia - historical overview and current concept. *Acta Neurochir.* **144**, 649–664, DOI: 10.1007/s00701-002-0944-3 (2002).

6. du Boulay, G., Shah, S. H., Currie, J. C. & Logue, V. The mechanism of hydromyelia in Chiari type 1 malformations. *The Br. J. Radiol.* **47**, 579–587, DOI: 10.1259/0007-1285-47-561-579 (1974).

7. Heiss, J. D. *et al.* Elucidating the pathophysiology of syringomyelia. *J. Neurosurg.* **91**, 553–562, DOI: 10.3171/jns.1999.91.4.0553 (1999).

8. Milhorat, T. H., Miller, J. I., Johnson, W. D., Adler, D. E. & Heger, I. M. Anatomical basis of syringomyelia occurring with hindbrain lesions. *Neurosurgery* **32**, 748–754; discussion 754, DOI: 10.1227/00006123-199305000-00008 (1993).

9. Stoodley, M. A. Pathophysiology of syringomyelia. *J. Neurosurg.* **92**, 1069–1070; author reply 1071–1073 (2000).

10. Terae, S., Miyasaka, K., Abe, S., Abe, H. & Tashiro, K. Increased pulsatile movement of the hindbrain in syringomyelia associated with the Chiari malformation: Cine-MRI with presaturation bolus tracking. *Neuroradiology* **36**, 125–129 (1994).

11. Chang, H. S. & Nakagawa, H. Hypothesis on the pathophysiology of syringomyelia based on simulation of cerebrospinal fluid dynamics. *J. Neurol. Neurosurgery, Psychiatry* **74**, 344–347 (2003).

12. Chang, H. S. & Nakagawa, H. Theoretical analysis of the pathophysiology of syringomyelia associated with adhesive arachnoiditis. *J. Neurol. Neurosurgery, Psychiatry* **75**, 754–757 (2004).

13. Greitz, D. Unraveling the riddle of syringomyelia. *Neurosurg. Rev.* **29**, 251–263; discussion 264, DOI: 10.1007/s10143-006-0029-5 (2006).

14. Ellertsson, A. B. Syringomyelia and other cystic spinal cord lesions. *Acta Neurol. Scand.* **45**, 403–417, DOI: 10.1111/j.1600-0404.1969.tb01254.x (1969).

15. Ellertsson, A. B. & Greitz, T. Myelocystographic and fluorescein studies to demonstrate communication between intramedullary cysts and the cerebrospinal fluid space. *Acta Neurol. Scand.* **45**, 418–430 (1969).

16. Li, K. C. & Chui, M. C. Conventional and CT metrizamide myelography in Arnold-Chiari I malformation and syringomyelia. *AJNR. Am. journal neuroradiology* **8**, 11–17 (1987 Jan-Feb).

17. Heiss, J. D. *et al.* Origin of Syrinx Fluid in Syringomyelia: A Physiological Study. *Neurosurgery* **84**, 457–468, DOI: 10.1093/neuros/nyy072 (2019).

18. Koyanagi, I. *et al.* Surgical treatment supposed natural history of the tethered cord with occult spinal dysraphism. *Child's Nerv. Syst. ChNS: Off. J. Int. Soc. for Pediatr. Neurosurg.* **13**, 268–274, DOI: 10.1007/s003810050081 (1997).

19. Wolpert, S. M., Bhadelia, R. A., Bogdan, A. R. & Cohen, A. R. Chiari I malformations: Assessment with phase-contrast velocity MR. *AJNR. Am. journal neuroradiology* **15**, 1299–1308 (1994).

20. Bhadelia, R. A. *et al.* Cerebrospinal fluid flow waveforms: Analysis in patients with Chiari I malformation by means of gated phase-contrast MR imaging velocity measurements. *Radiology* **196**, 195–202, DOI: 10.1148/radiology.196.1.7784567 (1995).

21. Hofmann, E., Warmuth-Metz, M., Bendszus, M. & Solymosi, L. Phase-contrast MR imaging of the cervical CSF and spinal cord: Volumetric motion analysis in patients with Chiari I malformation. *AJNR. Am. journal neuroradiology* **21**, 151–158 (2000).

22. Quigley, M. F., Iskandar, B., Quigley, M. E., Nicosia, M. & Haughton, V. Cerebrospinal fluid flow in foramen magnum: Temporal and spatial patterns at MR imaging in volunteers and in patients with Chiari I malformation. *Radiology* **232**, 229–236, DOI: 10.1148/radiol.2321030666 (2004).

23. Klekamp, J., Batzdorf, U., Samii, M. & Bothe, H. W. Treatment of syringomyelia associated with arachnoid scarring caused by arachnoiditis or trauma. *J. Neurosurg.* **86**, 233–240, DOI: 10.3171/jns.1997.86.2.0233 (1997).

24. Brodbelt, A. R. *et al.* Altered subarachnoid space compliance and fluid flow in an animal model of posttraumatic syringomyelia. *Spine* **28**, E413–419, DOI: 10.1097/01.BRS.0000092346.83686.B9 (2003).

25. Heiss, J. D. *et al.* Pathophysiology of primary spinal syringomyelia. *J. Neurosurgery. Spine* **17**, 367–380, DOI: 10.3171/2012.8.SPINE111059 (2012).

26. Chang, H. S., Nagai, A., Oya, S. & Matsui, T. Dorsal spinal arachnoid web diagnosed with the quantitative measurement of cerebrospinal fluid flow on magnetic resonance imaging. *J. Neurosurgery. Spine* **20**, 227–233, DOI: 10.3171/2013.10.SPINE13395 (2014).

27. Stoodley, M. A., Jones, N. R., Yang, L. & Brown, C. J. Mechanisms underlying the formation and enlargement of noncommunicating syringomyelia: Experimental studies. *Neurosurg. Focus.* **8**, 1–7, DOI: 10.3171/foc.2000.8.3.2 (2000).

28. Chang, H. S. Hypothesis on the pathophysiology of syringomyelia based on analysis of phase-contrast magnetic resonance imaging of Chiari-I malformation patients, DOI: 10.12688/f1000research.72823.1 (2021).

29. Elliott, N. S. J., Bertram, C. D., Martin, B. A. & Brodbelt, A. R. Syringomyelia: A review of the biomechanics. *J. Fluids Struct.* **40**, 1–24, DOI: 10.1016/j.jfluidstructs.2013.01.010 (2013).

30. Serway, R. A. Fluids and Solids. In *College Physics*, 267–319 (Cengage Learning, Boston, 2016), eleventh edn.

31. Davis, C. H. & Symon, L. Mechanisms and treatment in post-traumatic syringomyelia. *Br. J. Neurosurg.* **3**, 669–674, DOI: 10.3109/02688698908992690 (1989).

32. Ellertsson, A. B. & Greitz, T. The distending force in the production of communicating syringomyelia. *Lancet (London, England)* **1**, 1234, DOI: 10.1016/s0140-6736(70)91829-5 (1970).

33. Shi, Y., Lawford, P. & Hose, R. Review of Zero-D and 1-D Models of Blood Flow in the Cardiovascular System. *BioMedical Eng. OnLine* **10**, 33, DOI: 10.1186/1475-925X-10-33 (2011).

34. Kokalari, I., Karaja, T. & Guerrisi, M. Review on lumped parameter method for modeling the blood flow in systemic arteries. *J Biomed Sci Eng* **6**, 92–99 (2013).

35. Brook, B. S., Falle, S. & Pedley, T. J. Numerical solutions for unsteady gravity-driven flows in collapsible tubes: Evolution and roll-wave instability of a steady state. *J. Fluid Mech.* **396**, 223–256 (1999).

36. Sherwin, S. J., Formaggia, L., Peiro, J. & Franke, V. Computational modelling of 1D blood flow with variable mechanical properties and its application to the simulation of wave propagation in the human arterial system. *Int. journal for numerical methods fluids* **43**, 673–700 (2003).

37. Huilgol, R. R. & Georgiou, G. C. A fast numerical scheme for the Poiseuille flow in a concentric annulus. *J. Non-Newtonian Fluid Mech.* **285**, 104401, DOI: 10.1016/j.jnnfm.2020.104401 (11 1, 2020).

38. Williams, B. Simultaneous cerebral and spinal fluid pressure recordings. 2. Cerebrospinal dissociation with lesions at the foramen magnum. *Acta Neurochir.* **59**, 123–142, DOI: 10.1007/BF01411198 (1981).

39. Newman, P. K., Terenty, T. R. & Foster, J. B. Some observations on the pathogenesis of syringomyelia. *J. Neurol. Neurosurgery, Psychiatry* **44**, 964–969, DOI: 10.1136/jnnp.44.11.964 (1981).

40. Yasui, K., Hashizume, Y., Yoshida, M., Kameyama, T. & Sobue, G. Age-related morphologic changes of the central canal of the human spinal cord. *Acta Neuropathol.* **97**, 253–259 (1999).